The Astrophysical Journal Letters, 775:L32 (6pp), 2013 September 20 doi:10.1088/2041-8205/775/1/L32

ANTI-PARALLEL EUV FLOWS OBSERVED ALONG ACTIVE REGION FILAMENT THREADS WITH HI-C

Caroline E. Alexander[1], Robert W. Walsh[1], Stéphane Régnier[1], Jonathan Cirtain[2], Amy R. Winebarger[2], Leon Golub[3], Ken Kobayashi[4], Simon Platt[5], Nick Mitchell[5], Kelly Korreck[3], Bart DePontieu[6], Craig DeForest[7], Mark Weber[3], Alan Title[6], and Sergey Kuzin[8]
[1] Jeremiah Horrocks Institute, University of Central Lancashire, Preston PR1 2HE, UK
[2] NASA Marshall Space Flight Center, VP 62, Huntsville, AL 35812, USA
[3] Harvard-Smithsonian Center for Astrophysics, 60 Garden Street, Cambridge, MA 02138, USA
[4] Center for Space Plasma and Aeronomic Research, The University of Alabama in Huntsville, 320 Sparkman Drive, Huntsville, AL 35805, USA
[5] School of Computing, Engineering and Physical Sciences, University of Central Lancashire, Preston PR1 2HE, UK
[6] Lockheed Martin Solar & Astrophysics Lab, 3251 Hanover Street, Org. ADBS, Bldg. 252, Palo Alto, CA, USA
[7] Southwest Research Institute, 1050 Walnut Street, Suite 300, Boulder, CO 80302, USA
[8] P.N. Lebedev Physical institute of the Russian Academy of Sciences, Leninskii prospekt, 53, 119991 Moscow, Russia
Received 2013 June 20; accepted 2013 August 24; published 2013 September 10

ABSTRACT

Plasma flows within prominences/filaments have been observed for many years and hold valuable clues concerning the mass and energy balance within these structures. Previous observations of these flows primarily come from Hα and cool extreme-ultraviolet (EUV) lines (e.g., 304 Å) where estimates of the size of the prominence threads has been limited by the resolution of the available instrumentation. Evidence of "counter-steaming" flows has previously been inferred from these cool plasma observations, but now, for the first time, these flows have been directly imaged along fundamental filament threads within the million degree corona (at 193 Å). In this work, we present observations of an AR filament observed with the High-resolution Coronal Imager (Hi-C) that exhibits anti-parallel flows along adjacent filament threads. Complementary data from the *Solar Dynamics Observatory* (*SDO*)/Atmospheric Imaging Assembly (AIA) and Helioseismic and Magnetic Imager are presented. The ultra-high spatial and temporal resolution of Hi-C allow the anti-parallel flow velocities to be measured (70–80 km s^{-1}) and gives an indication of the resolvable thickness of the individual strands ($0\farcs8 \pm 0\farcs1$). The temperature of the plasma flows was estimated to be $\log T\,(\mathrm{K}) = 5.45 \pm 0.10$ using Emission Measure loci analysis. We find that *SDO*/AIA cannot clearly observe these anti-parallel flows or measure their velocity or thread width due to its larger pixel size. We suggest that anti-parallel/counter-streaming flows are likely commonplace within all filaments and are currently not observed in EUV due to current instrument spatial resolution.

Key words: Sun: corona – Sun: filaments, prominences

Online-only material: color figures, animation

1. INTRODUCTION

Research on the mechanisms that create and maintain solar prominences has benefited greatly in recent years from the increased resolution of instrumentation. High resolution observations of both filaments (on-disk) and prominences (off-limb) give crucial insight into the mass maintenance and magnetic field structure that is needed to fully comprehend how these cool, dense structures form and survive within the corona.

Prominences are formed from individual threads and knots of mass (Engvold 1976) that are suspended within the magnetic field of the corona. They are typically 100 times cooler and denser than the coronal average (Labrosse et al. 2010) and are formed over polarity inversion lines (PIL; Babcock & Babcock 1955). The role of the magnetic field in structuring filament material can be examined by mapping the flow of plasma along field-aligned filament threads. These flows can highlight the anatomy of the magnetic field and could be used to test the veracity of many of the current models (see, e.g., Mackay et al. 2010 for a comprehensive review).

The majority of observations that examine prominence threads are taken in Hα which typically yield spatial resolutions higher than have been achievable in the extreme-ultraviolet (EUV) and X-ray. Lin et al. (2005) used data from the Swedish Solar Telescope and found that filament threads had an average width of $0\farcs3$ but postulated that since this was near the instrument's resolution, finer structures were likely to exist. EUV observations have shown that the higher temperature components of filaments are wider than their Hα counterparts due to absorption by the hydrogen Lyman continuum (Heinzel et al. 2001; Schmieder et al. 2004). This may have an impact on the fundamental scale that these threads can be measured to at EUV wavelengths.

Zirker et al. (1998) first coined the term "counter-streaming" to describe the bi-directional pattern of flows observed within filaments. These motions (see also, e.g., Engvold 1976; Lin et al. 2003, 2005; Chae et al. 2007; Schmieder et al. 2008; Panasenco & Martin 2008) highlight a more complex picture of prominence dynamics and can give clues to the physical scale of the fundamental prominence threads as well as the source of the mass flows.

The counter-streaming flows examined by Zirker et al. (1998) were observed in the wings of the Hα line as both redshifts and blueshifts, indicating that plasma was flowing both toward and away from the observer. A similar motion was observed perpendicular to the line of sight along the threads of the prominence spine.

The work presented here details ultra-high resolution EUV observations of counter-streaming flows along filament threads observed with NASA's High-resolution Coronal Imager (Hi-C).

It is the first observation of anti-parallel flows along adjacent filament threads in the EUV. We make the distinction between the general term "counter-streaming" and the more specific "anti-parallel" flows, which we define as mass flows in opposite directions observed along adjacent filament threads. These are localized flows that can be biased in one direction as opposed to counter-streaming flows, which typically describe plasma motion along filament threads with an equal distribution in up/down or east/west directions (see, e.g., Zirker et al. 1998; Lin et al. 2003; Ahn et al. 2010).

Section 2 gives a brief outline of the Hi-C instrument and the data used in this study. Section 3 details our results concerning (1) the photospheric magnetic environment of the filament, (2) the width of the prominence threads, (3) the velocity of the plasma flows along the threads, and (4) the temperature profile of these flows. Section 4 presents the conclusions gathered from our analysis of this data set.

2. OBSERVATIONS AND DATA ANALYSIS

The Hi-C (Cirtain et al. 2013; Kobayashi et al. 2013) is a new instrument developed by NASA's Marshall Space Flight Center and partners[9] that was launched on a sounding rocket at approximately 18:50 UT on 2012 July 11. The instrument imaged a large, magnetically complicated active region (AR 11520) with the highest degree of spatial resolution ever achieved in the EUV wavelength regime.

Hi-C has a pixel size of 0.″1 and its primary mirror has a diameter of 240 mm which together give Hi-C a spatial resolution of ∼0.″3. Comparing this with the 0.″6 pixel size and 1.″2 resolution of *Solar Dynamics Observatory*/Atmospheric Imaging Assembly (*SDO*/AIA; Lemen et al. 2012), Hi-C offers about four times higher resolution. The cadence of Hi-C was ∼5.5 s compared to *SDO*/AIA's 12 s. AR 11520 was imaged by Hi-C for approximately 5 minutes and resulted in 200 s of high-quality data for the field of view (FOV) (7.′1 × 7.′0) shown in Figure 1 (top left panel).

The Hi-C optics were designed to image a narrow wavelength region around 193 Å which is dominated by the Fe XII 195.119 Å line, formed at 1.5 MK. The temperature response of Hi-C (from SSW routine HIC_GET_RESPONSE.PRO) is very similar to the *SDO*/AIA 193 Å channel (see Figure 2). The *SDO*/AIA temperature response function was calculated using the CHIANTI (v7.1; Landi et al. 2013) "Isothermal" routine with "coronal" abundances, standard ionization equilibrium, and a density of 10^{10} cm^{-3}. It can be seen that both functions cover the same temperature regions with the same peaks and troughs in sensitivity.

Figure 1 shows the context and location of the filament under investigation in Hi-C as well as co-aligned data from *SDO*/AIA (193 Å, 304 Å, and 4500 Å), BBSO/Hα, and *SDO*/Helioseismic and Magnetic Imager (HMI). Information from additional *SDO*/AIA filters (94 Å, 131 Å, 171 Å, 193 Å, 211 Å, and 335 Å) was also utilized in the analysis of these flows.

3. RESULTS

The nature of the anti-parallel flows observed in the small AR filament has been explored by investigating the magnetic environment of the filament, the physical width of the filament threads, the velocity of the mass flows along these threads, and the temperature profile of the plasma that makes up these flows.

[9] See the acknowledgements.

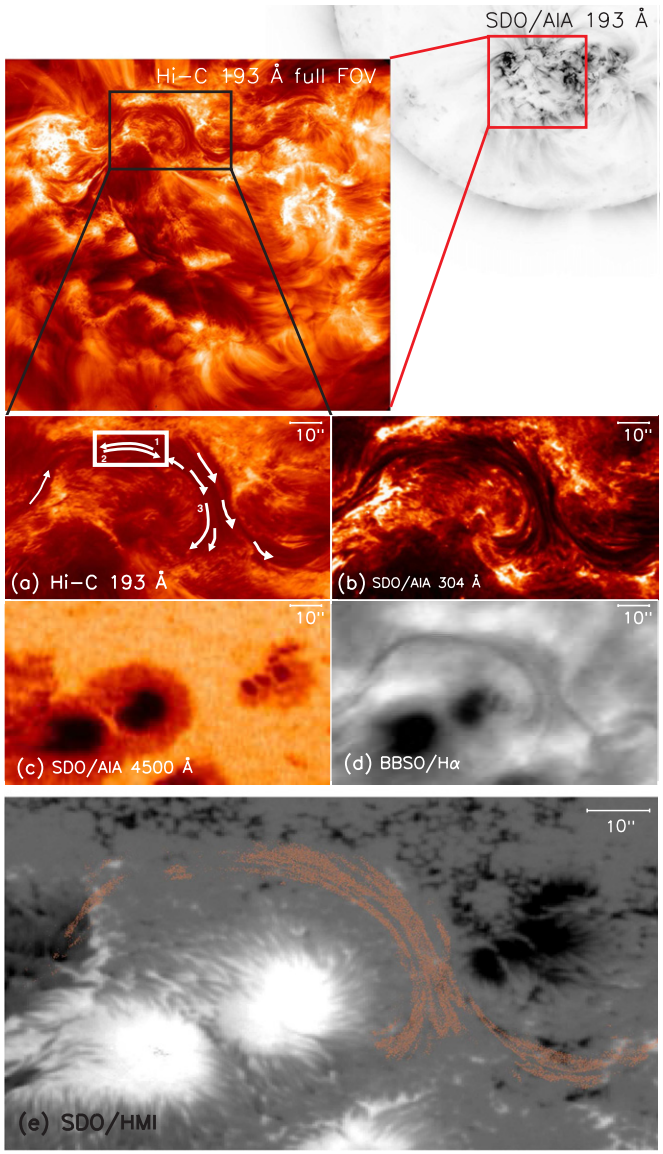

Figure 1. Top right: partial full-disk image of the Sun taken with *SDO*/AIA 193 Å to show AR 11520 in context at 18:56 UT on the 2012 July 11. The box highlights the FOV of Hi-C and the top left image shows an example Hi-C frame (at 18:55:16 UT) where the black box shows the location of the small filament. The four central images and the bottom image show this FOV in various co-aligned observations: (a) Hi-C 193 Å with the pattern of the flows indicated by the arrows. The numbers highlight flows that were examined and the white box shows the location of the anti-parallel flows (see the online animation). (b) *SDO*/AIA 304 Å image shows the filament at a lower temperature (∼50,000 K). (c) *SDO*/AIA 4500 Å image (taken at 17:00 UT) shows the location of the nearby sunspots in relation to the filament. (d) BBSO image of the filament in Hα (2012 July 10, 23:30:08 UT). (e) *SDO*/HMI shows the magnetic environment of the filament with Hi-C contours overlaid to show the position of the filament.

(An animation and a color version of this figure are available in the online journal.)

3.1. Magnetic Structure

AR 11520 is a magnetically complex, decaying active region. The filament under observation is located in the middle of this region wrapped around a sunspot (Figure 1(c)) and over a PIL (Figure 1(e)). The filament material is observed clearly in Hα (Figure 1(d)) which shows that the filament has a two-part structure (i.e., the main body curving around the sunspot and an additional component seen to branch off toward the west).

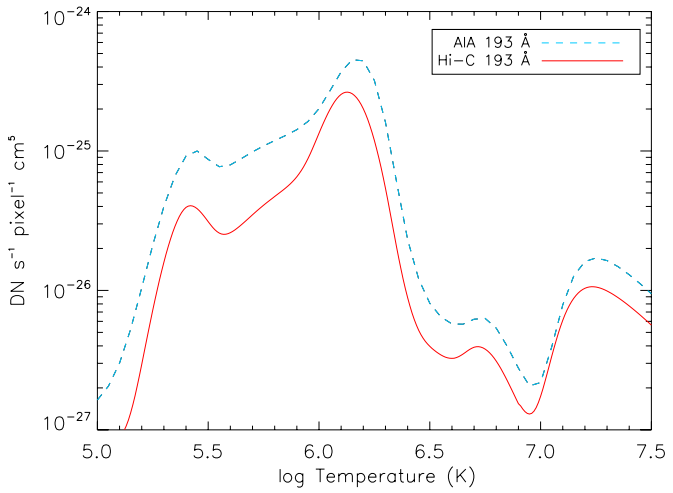

Figure 2. Comparison between the temperature response functions of *SDO*/AIA 193 Å and Hi-C. Note that the pixel^{-1} aspect of the response units refers to different sizes for the two instruments.

(A color version of this figure is available in the online journal.)

The plasma flows observed with Hi-C travel along the spine of the filament with the majority of the flows traveling west (shown by the arrows in Figure 1(a)). This suggests that the eastward flows may be contained within a small subset of strands along the main filament body.

Flows of material within filaments can give clues about the magnetic field structure in and around these features (Mackay et al. 2010). However, caution must be exercised as the higher density of these structures means that these flows are not necessarily aligned with the magnetic field, i.e., plasma is not "frozen into" the magnetic field any longer. With this in mind, we suggest that these flows infer that the magnetic field is horizontal along the spine of the filament but note that this does not shed any light on the structure of the surrounding magnetic field supporting the filament.

The HMI photospheric magnetogram in Figure 1(e) shows the position of the filament, overlaid in Hi-C contours, with respect to the PIL and surrounding magnetic field. Along the edge of the PIL, multiple instances of magnetic flux convergence and subsequent cancellation were observed and attributed to the interaction between the dominant polarities on either side of the PIL and areas of parasitic flux (i.e., smaller portions of weaker flux with a polarity opposite to the dominant polarity in a particular location). Various authors (see, e.g., Martin & Echols 1994; Wang & Muglach 2007) suggest that these sites are associated with the "footpoints" of filaments, i.e., areas where the structure is rooted to the photosphere.

Multiple footpoints could be responsible for the difference in flow direction observed within the central part of the filament (white box, Figure 1(a)). If the anti-parallel flows are in fact rooted in different polarity pairs, there could be a marked difference in, say, any rate of magnetic reconnection and chromospheric evaporation taking place at each site. This in turn could influence the direction and nature of the plasma flows.

We interpret these flows as evidence of cool mass injection from the chromosphere due to heating caused by magnetic reconnection at the footpoints. This plasma is viewed moving horizontally along the filament spine and we suggest that these anti-parallel flows are not a special case scenario. Their particular orientation in this active region coupled with the high spatial resolution of Hi-C is the reason they are observed here for the first time.

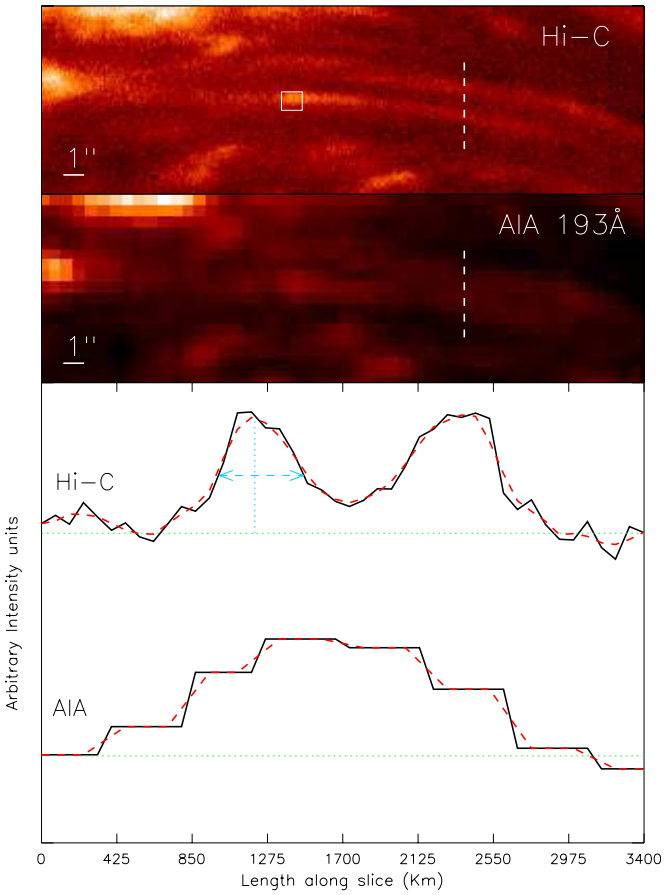

Figure 3. Two top images show the FOV where the anti-parallel flows are observed (white box, Figure 1(a)) imaged by Hi-C and *SDO*/AIA 193 Å at 18:53:35 UT. The intensity in these images was measured along the dashed white lines and plotted in the bottom panel. The black line in each case represents the intensity along this cut (averaged over 10 Hi-C pixels and 2 *SDO*/AIA pixels, respectively), the dashed line (red) is the smoothed intensity, the dotted line (green) is the background intensity, and the blue dashed line represents the FWHM of one of the Hi-C peaks, which we define as the width of the thread. The white box in the upper image is the region used for temperature analysis in the next section.

(A color version of this figure is available in the online journal.)

3.2. Thread Width

The fine-scale structure of the filament threads is an important factor to determine. The anti-parallel flows along the filament are observed with Hi-C and some anti-parallel motion may be seen in *SDO*/AIA 193 Å and 304 Å images, but it is not clearly discernible (even with image enhancement) and we note that it would not be identifiable without Hi-C as a guide.

The width of the two adjacent threads exhibiting anti-parallel flows is examined in Figure 3. The top portion of this figure shows the flows seen by Hi-C and *SDO*/AIA 193 Å where the dashed vertical lines indicate cuts that were taken to examine the width of the threads. The larger pixel size of *SDO*/AIA is clearly seen. The lower panel of this figure shows the intensity profile along the cuts in each case. These profiles show that the two threads are clearly identified by Hi-C but are merged into one structure by the larger pixel size of *SDO*/AIA.

We define the physical width of the threads as the FWHM of this intensity profile (blue dashed line) and this is found to be

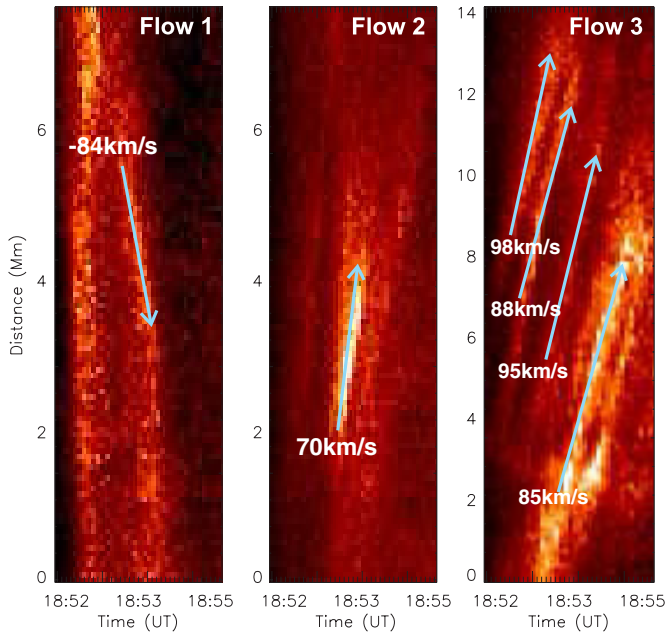

Figure 4. Time–distance plots of flows seen along arrows 1, 2, and 3 in Figure 1(a). The anti-parallel flows are seen in the left and middle panels while multiple mass flows are seen in the right panel representing the flow observed to move around the edge of the sunspot.

(A color version of this figure is available in the online journal.)

0.″8 ± 0.″1. The gap between the threads was of a similar width (0.″9). This provides a strong indication that Hi-C has resolved fundamentally coherent structures at this wavelength. This is further validated by the number of Hi-C pixels contained within each thread's intensity peak (7–9) which shows this is a clear structure well within the resolution of the instrument. This strand width is comparable to the width of the other threads within the filament. The coherence of the anti-parallel flows will be further investigated by examining the speed of the plasma flows.

3.3. Velocity

The flows labeled 1–3 in Figure 1(a) were investigated further by constructing time–distance plots of intensity (in pixels indicated by the arrow positions) over the 200 s of Hi-C data available. Additional flows were observed along the filament but were not measurable as time–distance plots due to background noise. Figure 4 shows these time–distance plots with the observed flows and velocities highlighted.

It can be seen in Figure 4 that flows 1 and 2 are anti-parallel and of the same order (-84.2 ± 15.3 km s^{-1} and 70.2 ± 15.6 km s^{-1}, respectively). Flow "3" (as labeled in Figure 1(a)) was also examined and was seen to exhibit multiple mass flows over the time series indicated by numerous diagonal signatures on the time–distance plot.

The magnitude of these uni-directional velocity flows are of the same order as flows 1 and 2, suggesting that the anti-parallel flows observed have a typical flow speed for this filament. Flow speeds measured by other authors in Hα are corresponding slower, e.g., 5–20 km s^{-1} (Zirker et al. 1994) due to the lower temperature/higher density of plasma imaged in this wavelength.

The larger pixel size of *SDO*/AIA meant that any signatures were lost in the background intensity and thus no measurement of velocity was possible without Hi-C.

3.4. Temperature

SDO/AIA provides valuable context for analysis of the Hi-C observations and allows the active region filament to be viewed over numerous wavelengths, thereby allowing information regarding the filament's temperature to be examined. Data from eight *SDO*/AIA channels (94 Å, 131 Å, 171 Å, 193 Å, 211 Å, 304 Å, 335 Å, and 1600 Å) was employed to determine how the intensity of the flows changed when viewed in different filters. A small region on one of the strands exhibiting anti-parallel flows was chosen for investigation (Figure 3, white box). The left panel of Figure 5 shows normalized light curves in five of these *SDO*/AIA channels (plus Hi-C), which exhibited a peak in intensity (channels 94 Å, 211 Å, and 335 Å exhibited a flat intensity profile over the time series).

Six filters exhibited a peak in intensity at around 18:53:35 UT (dotted line in left panel of Figure 5) with the spread of the peaks being ±10 s around this time. Since the temporal cadence of *SDO*/AIA is 12 s, it is not possible to quantify each filter's peak emission time with more accuracy; thus we consider these peaks co-temporal within the instrumental constraints.

This co-temporal intensity peak suggests that either the plasma is very multi-thermal or is isothermal at a temperature at which all of these filters are sensitive. It is very likely this is a mass flow as opposed to a heating event creating a conduction front as the peaks would occur in a clear order with a time lag in between (see, e.g., Viall & Klimchuk 2011) if this was the case.

The temperature of these flows was further investigated using the Emission Measure (EM) loci method (see, e.g., Del Zanna et al. 2002). The constructed plot is shown in the right panel of Figure 5 and was made using the same intensity values gathered from the region highlighted by the small white box in Figure 3.

The *SDO*/AIA temperature response functions were calculated using the method described by Del Zanna et al. (2011; see Section 2). Caution must be exercised when using imager data for this type of analysis as there are a number of well-known problems with some of the *SDO*/AIA filters, e.g., cross-talk, unidentified lines, and second-order contributions (see, e.g., O'Dwyer et al. 2010; Del Zanna et al. 2011; Boerner et al. 2012). The four filters used for EM loci analysis were selected as they showed a peak in intensity at this time and are not representative of transition region plasma (as the *SDO*/AIA 304 Å and 1600 Å are).

It can be seen that the four curves cross within the area highlighted by the dashed black box. The middle of this box is found to be at $\log T\,(\mathrm{K}) = 5.45 \pm 0.1$. This temperature is higher than the average temperature of filament material which is of the order of 10^4 K (Labrosse et al. 2010).

4. DISCUSSION AND CONCLUSIONS

This work has highlighted anti-parallel flows observed along adjacent filament threads as seen by Hi-C. It has been shown that although *SDO*/AIA gives valuable context and multi-wavelength observations, the instrument cannot identify these small-scale flows or measure their width or velocity. This work, as well as additional work using Hi-C (see Cirtain et al. 2013; Testa et al. 2013; Morton & McLaughlin 2013; Winebarger et al. 2013; Régnier et al. 2013), has explicitly shown that Hi-C captured phenomena never seen before and which cannot be properly examined using current instrumentation.

The pattern of flows seen along the filament suggests that the flows are closely related to the magnetic footpoints of the structure. It is likely that the two threads exhibiting anti-parallel

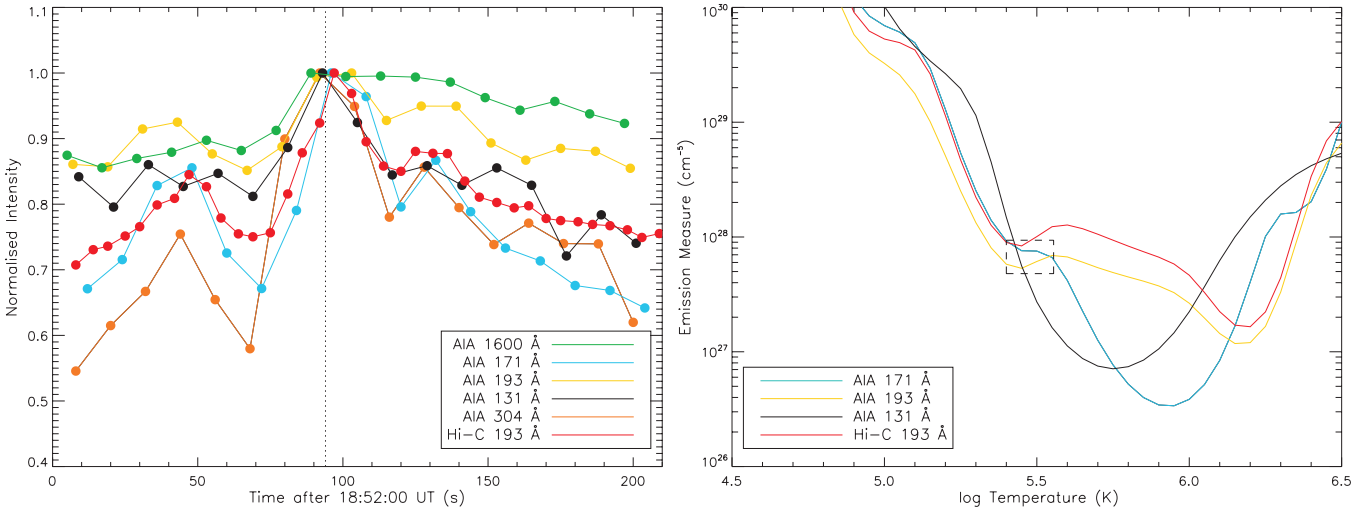

Figure 5. Left: normalized light curves of the intensity change over time based in the area in the white box in the top panel of Figure 3. It can be seen that all six filters peak in the same 5–10 s period indicated by the vertical dotted line. Right: EM loci curves made using Hi-C and various *SDO*/AIA EUV passbands for data taken at 18:53:35 UT. The black dashed line box indicates the area where the most crossings occur and indicates a plasma temperature of log $T = 5.45 \pm 0.10$.

(A color version of this figure is available in the online journal.)

flows are separate sub-structures within the filament as the coherence of the velocity flows suggests the plasma is flowing along different flux tubes. The flows travel horizontally along the spine of the filament, but we have no information about the inclination of the individual threads so cannot comment on the overall structure of the magnetic field.

Measuring the width of the filament threads established that the structures are spatially coherent. However, it is the velocity coherence that demonstrates that these anti-parallel flows are contained within separate sub-structures. Furthermore, it is possible these separate threads are "bundles" of smaller-scale thread-like structures exhibiting the same pattern of mass flows.

Based on the calculated velocities, these anti-parallel flows are similar to other flows observed within the filament, suggesting that they are not a special case and therefore may be ubiquitous within all filaments/prominences.

The temperature of one of the flows is indicated to be $\log T\,(\mathrm{K}) = 5.45 \pm 0.10$ ($\sim$280,000 K), which is supported by the intensity enhancements seen in the cooler *SDO*/AIA 304 Å and 1600 Å filters. This temperature, however, is higher than expected considering the filament's observation in Hα ($T \leqslant 10^4$ K; Aulanier & Schmieder 2002). We suggest that the filament observed by Hi-C is most likely multi-layered with components at different atmospheric heights. This measurement highlights the possibility of there being temperature transition regions around filament threads (i.e., a hotter transition region around cooler filament threads) and gives an important insight into the filament's environment.

Studying small-scale filament flows such as those observed by Hi-C can give valuable information concerning fundamental questions such as the source and sinks of the mass flows, as well as the orientation of the magnetic field within these structures. From these observations, it seems the magnetic field within this filament is parallel to the solar disk rather than helical in nature, which can impact many of the current models on prominence structure.

This is the first direct subarcsecond observation of anti-parallel/counter-streaming flows along filament threads at EUV wavelengths and showcases the power of Hi-C's higher spatial and temporal resolution. Future work will expand upon this analysis by incorporating modeling of the filament magnetic field using *SDO*/HMI data. This will allow us to comment further on the origin of the anti-parallel flows and also to extend this work to other examples.

C.E.A. thanks Olga Panasenco and Giulio Del Zanna for very useful discussions. We also thank the referee for useful comments. MSFC/NASA led the mission and partners include the Smithsonian Astrophysical Observatory in Cambridge, Massachusetts; Lockheed Martin's Solar Astrophysical Laboratory in Palo Alto, California; the University of Central Lancashire in Lancashire, England; and the Lebedev Physical Institute of the Russian Academy of Sciences in Moscow. CHIANTI is a collaborative project involving George Mason University, the University of Michigan (USA), and the University of Cambridge (UK).

REFERENCES

Ahn, K., Chae, J., Cao, W., & Goode, P. R. 2010, ApJ, 721, 74
Aulanier, G., & Schmieder, B. 2002, A&A, 386, 1106
Babcock, H. W., & Babcock, H. D. 1955, ApJ, 121, 349
Boerner, P., Edwards, C., Lemen, J., et al. 2012, SoPh, 275, 41
Chae, J., Park, H.-M., & Park, Y.-D. 2007, JKAS, 40, 67
Cirtain, J. W., Golub, L., Winebarger, A. W., et al. 2013, Natur, 493, 501
Del Zanna, G., Landini, M., & Mason, H. E. 2002, A&A, 385, 968
Del Zanna, G., O'Dwyer, B., & Mason, H. E. 2011, A&A, 535, A46
Engvold, O. 1976, SoPh, 49, 283
Heinzel, P., Schmieder, B., & Tziotziou, K. 2001, ApJL, 561, L223
Kobayashi, K., Cirtain, J. W., Golub, L., et al. 2013, SoPh, submitted
Labrosse, N., Heinzel, P., Vial, J.-C., et al. 2010, SSRv, 151, 243
Landi, E., Young, P. R., Dere, K. P., Del Zanna, G., & Mason, H. E. 2013, ApJ, 763, 86
Lemen, J. R., Title, A. M., Akin, D. J., et al. 2012, SoPh, 275, 17
Lin, Y., Engvold, O., Rouppe van der Voort, L., Wiik, J. E., & Berger, T. E. 2005, SoPh, 226, 239
Lin, Y., Engvold, O. R., & Wiik, J. E. 2003, SoPh, 216, 109
Mackay, D. H., Karpen, J. T., Ballester, J. L., Schmieder, B., & Aulanier, G. 2010, SSRv, 151, 333
Martin, S. F., & Echols, C. R. 1994, in Solar Surface Magnetism, ed. R. J. Rutten & C. J. Schrijver (Dordrecht: Kluwer), 339
Morton, R. J., & McLaughlin, J. A. 2013, A&A, 553, L10
O'Dwyer, B., Del Zanna, G., Mason, H. E., Weber, M. A., & Tripathi, D. 2010, A&A, 521, A21

Panasenco, O., & Martin, S. F. 2008, in ASP Conf. Ser. 383, Subsurface and Atmospheric Influences on Solar Activity, ed. R. Howe, R. W. Komm, K. S. Balasubramaniam, & G. J. D. Petrie (San Francisco, CA: ASP), 243
Régnier, S., Alexander, C. E., Walsh, R. W., et al. 2013, ApJ, submitted
Schmieder, B., Bommier, V., Kitai, R., et al. 2008, SoPh, 247, 321
Schmieder, B., Lin, Y., Heinzel, P., & Schwartz, P. 2004, SoPh, 221, 297
Testa, P., De Pontieu, B., Martínez-Sykora, J., et al. 2013, ApJL, 770, L1
Viall, N. M., & Klimchuk, J. A. 2011, ApJ, 738, 24
Wang, Y.-M., & Muglach, K. 2007, ApJ, 666, 1284
Winebarger, A. R., Walsh, R. W., Moore, R., et al. 2013, ApJ, 771, 21
Zirker, J. B., Engvold, O., & Martin, S. F. 1998, Natur, 396, 440
Zirker, J. B., Engvold, O., & Yi, Z. 1994, SoPh, 150, 81